JOURNAL OF SOLID STATE CHEMISTRY 117, 73–79 (1995)

Physical Properties and Electronic Structure of Ternary Barium Copper Sulfides

Abdelkrim Ouammou, Mona Mouallem-Bahout, Octavio Peña, Jean-François Halet,[1] Jean-Yves Saillard, and Claude Carel[1]

Laboratoire de Chimie du Solide et Inorganique Moléculaire, URA CNRS 1495, Université de Rennes I, 35042 Rennes Cedex, France

Received June 24, 1994; in revised form December 13, 1994; accepted December 15, 1994

The electrical and magnetic properties of the tetragonal $BaCu_2S_2$ and orthorhombic α-$BaCu_4S_3$ compounds are reported as functions of temperature. The electrical resistivity measurements on pressed pellets show that both compounds are semiconductors. A diamagnetic behavior was found for the two compounds at $T > 70$ K, followed by a weak paramagnetic increase ($\mu_{eff} \leq 0.2\ \mu_B$) at lower temperatures. The electronic structure and bonding properties of stoichiometric $BaCu_2S_2$ and $BaCu_4S_3$ are analyzed by means of extended Hückel tight-binding calculations. The results suggest that both compounds adopt a semiconductor behavior, in agreement with the resistivity measurements. © 1995 Academic Press, Inc.

INTRODUCTION

The study of various copper-containing materials has recently received particular attention, stimulated by the discovery of the high-T_c superconductor copper oxides. A new investigation of the pseudo-binary Cu_2S–BaS system in our laboratory led to the preparation of the barium copper sulfides tetragonal $BaCu_2S_2$ and α-phase orthorhombic $BaCu_4S_3$ (1, 3). Following a preliminary note on their new preparation (5), we report in this paper the temperature-dependent electrical and magnetic behavior and the band electronic structure of $BaCu_2S_2$ and $BaCu_4S_3$.

EXPERIMENTAL

Initially, the structure of $BaCu_2S_2$ was determined from single crystal X ray diffraction data by Iglesias *et al.* in the 1970s (2, 3, 12) with space group *Pnma*. We prepared this compound in pure powder form (5) as described by Saeki *et al.* (6, 7). It was indexed on the basis of a tetragonal cell with the space group I_4/mmm which was found again by Savel'eva and colleagues (8). Therefore, it is likely a polymorph of the former. We were not able to obtain single crystals according to the preparation method given in Ref. (8). The typical composition resulting from an elementary analysis performed with scanning electron microscopy (SEM) was $Ba_{0.96}Cu_{2.05}S_{1.99}$.[2]

The α-phase $BaCu_4S_3$, called $BaCu_4S_3$ in the text, first studied by Steinfink *et al.* (1, 3, 4), was obtained in powder form using a new preparation method (5). Attempts to systematically vary this procedure in order to obtain single crystals have been unsuccessful thus far. A SEM analysis led to the chemical formula $Ba_{1.02}Cu_{3.97}S_{3.01}$.

The electrical resistivity measurements have been performed on pellets of 5 mm in diameter pressed at about 7 kbar, using the standard four-probe van der Pauw technique.

The magnetic susceptibility was measured from 5 K to room temperature under a 5-kOe magnetic field using a variable-temperature SQUID susceptometer (SHE-VTS-906). All the molecular and tight-binding (9) calculations were carried out within the extended Hückel formalism (10) using standard atomic parameters for Ba, Cu, and S. The exponent (ζ) and the valence shell ionization potential (H_{ii} in eV) were respectively 1.817, −20.0 for S 3*s*; 1.817, −13.3 for S 3*p*; 2.2, −11.4 for Cu 4*s*; 2.2, −6.06 for Cu 4*p*; and 1.214, −6.62 for Ba 6*s*; 1.214, −3.92 for Ba 6*p*. The H_{ii} for Cu 3*d* was set equal to −14.0 eV. A linear combination of two Slater-type orbitals of exponents $\zeta_1 = 5.95$ and $\zeta_2 = 2.1$ with weighting coefficients $c_1 = 0.577$ and $c_2 = 0.6167$ was used to represent the 3*d* atomic orbitals of Cu. Unless specified in text, all the considered interatomic distances are the experimental ones. The DOS of $BaCu_2S_2$ was obtained using a set of 40 *k* points taken in the irreducible part of the Brillouin zone corresponding to the tetragonal cell. The DOS of the three-dimensional $BaCu_4S_3$ compound was computed with a set of 12 *k* points

[1] To whom correspondence should be addressed.

[2] The formula was determined from an analysis performed on 30 to 50 1-μm^3 samples. The statistical confidence limit on the mean atomic percentage depends on the number of samples and ranges generally from less than 1 to 3% in the calculations.

0022-4596/95 $6.00

taken in the irreducible wedge of the Brillouin zone corresponding to the orthorhombic cell. All k point sets were chosen in accordance with the geometrical method described by Ramirez and Böhm (11).

RESULTS AND DISCUSSION

(a) *Description of the Structures*

A description of the structures of $BaCu_2S_2$ and $BaCu_4S_3$ compounds can be found in the literature (1–3, 8, 12, 14). They are briefly recalled here. $BaCu_2S_2$ adopts the well-known $ThCr_2Si_2$-type structure (I_4/mmm) (15). The refinement of our powder diffraction pattern leads to a = 3.908(1) Å, c = 12.656(2) Å, close to the values in Ref. (6). Analogous chalcogenides such as $KCuFeS_2$ and $KCuFeSe_2$ have recently been reported (16). For $BaCu_2S_2$, the Lazy Pulverix program using results published in (8) gives a simulated diffraction powder pattern fairly similar to the experimental one (5). In addition, experimental and calculated densities fit each other.

As shown in Fig. 1, this compound depicts a layered structure in which copper–sulfur slabs are separated by barium sheets. The Cu_2S_2 nets are anti-PbO-type layers, made of CuS_4 tetrahedra (Cu–S = 2.413 Å) sharing edges. In addition to the tetrahedral sulfur shell, each Cu atom lies in the middle of a square of copper congeners (Cu–Cu = 2.762 Å). The S atoms have a square-pyramidal geometry. An alternative way, to describe a Cu–S slab is to consider a square net of Cu atoms sandwiched in a staggered way by square nets of S atoms. The Ba cations are surrounded by a cube of S atoms (Ba–S = 3.267 Å).

Iglesias *et al.* have shown that α-$BaCu_4S_3$ crystallizes with the space group *Pnma* (1, 3). According to them, this compound can be prepared in pure form in a sealed tube. Attempts to reproduce their work lead only to a mixture of several phases, one of which is $BaCu_4S_3$. Our single-crystal measurements lead to an orthorhombic cell with parameters a = 10.752(3) Å, b = 4.028(3) Å, and c = 13.254(5) Å, comparable to those proposed earlier (1). A Lazy Pulverix simulation from the results in (1) gives a powder diffraction pattern in good agreement with that we obtained experimentally on our new prepared powder samples (5).

As shown in Fig. 2, $BaCu_4S_3$ adopts a three-dimensional structure containing infinite columns made up of BaS_6 trigonal prisms sharing triangular faces and running along the b direction (1, 3). The Ba–S distances vary from 3.120 to 3.307 Å. One square face of each BaS_6 prism is capped by a sulfur atom belonging to a prism of a neighboring column (Ba–S = 3.285 Å). These infinite "tubes" are held together by Cu atoms of different kinds (Cu(1–4)), which are either three- or fourfold coordinated to sulfur atoms in distorted Y-shaped (Cu(1) and Cu(2)) or tetrahedral (Cu(3) and Cu(4)) environments. The Cu–S separations range from 2.237 and 2.701 Å. Cu(1) and Cu(2) on one side and Cu(3) and Cu(4) on the other side form zigzag chains running parallel to the b direction (Cu(1)–Cu(2) = 2.754 Å and Cu(3)–Cu(4) = 2.677 Å). Quasi-linear chains made up of Cu(2) and Cu(3) run along the a axis (Cu(2)–Cu(3) = 2.573–2.850 Å). The structure of $BaCu_4S_3$ can be compared to that of anti-Re_3B (BaS_3), which would be distorted and stuffed with the copper atoms (3).

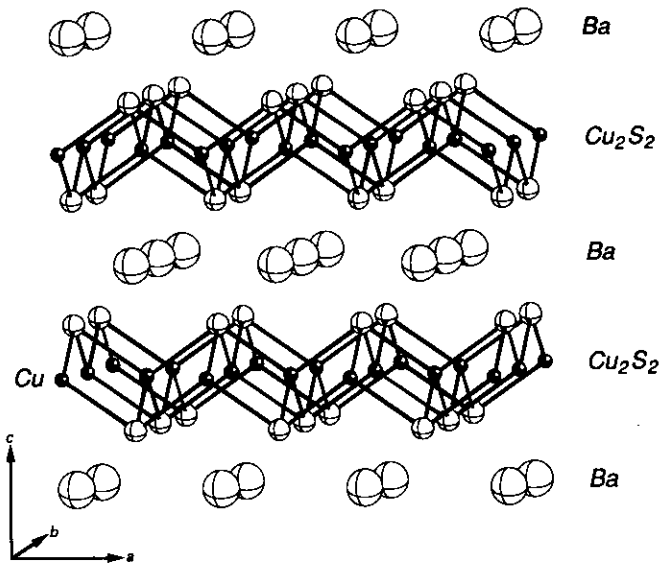

FIG. 1. Crystal structure of $BaCu_2S_2$.

(b) *Electrical Properties*

The curves $R_T/R_{290\,K} = f(T)$ illustrated in Fig. 3 for $BaCu_4S_3$ (curve 1) and $BaCu_2S_2$ (curve 2) in the temperature range 77–293 K are typical for semiconducting materials, though it was not possible to estimate the activation energy. The curve relating to $BaCu_4S_3$ obtained at present is quite similar to that given by Iglesias and Steinfink for α-$BaCu_4S_3$ in Fig. 1a in Ref. (4), particularly between 80 and 300 K. Note that Savel'eva and co-workers (8, 13, 14) have recently measured a metallic behavior for $BaCu_2S_2$ from room temperature to 40 K. This is somewhat surprising at first sight. When the Zintl concept is applied, the oxidation formalism appropriate for $BaCu_2S_2$ is $(Ba^{2+})[(Cu^{+})_2(S^{2-})_2]^{2-}$, leading to formal d^{10} Cu centers and consequently suggesting a semiconducting behavior for the material. In fact, it turns out that the preparation of pure $BaCu_2S_2$ proposed by Savel'eva *et al.* (8) leads to the formation of a mixture made of $Ba_{0.96}Cu_{2.01}S_{1.94}$ (85%) and $Ba_{0.95}Cu_{3.91}S_{2.97}$ (15%) (5). Being made of nonstoichiometric compounds deficient in barium (there are roughly 4% of Ba vacant sites in both compounds and 2% of Cu vacant sites in $BaCu_4S_3$), this mixture exhibits actually a metallic behavior until 77 K (5).

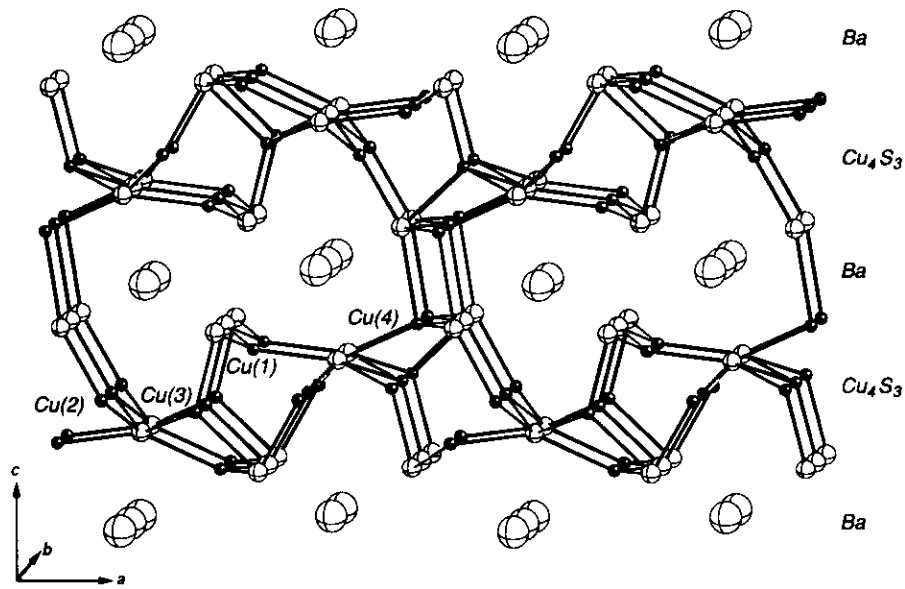

FIG. 2. Crystal structure of α-$BaCu_4S_3$.

(c) *Magnetic Properties*

The magnetic susceptibilities of $BaCu_2S_2$ and $BaCu_4S_3$ are shown in Figs. 4a and 4b, respectively. We found no indication for a superconducting behavior down to 2 K, in disagreement with a recent study, which suggests that both compounds could possibly be superconductors (17).

Negative values of the susceptibility were observed between 70 and 300 K (for $BaCu_2S_2$; Fig. 4a) and between 110 and 300 K (for $BaCu_4S_3$; Fig. 4b). At lower temperatures, a paramagnetic increase of the susceptibility is superposed to the diamagnetic component. In order to evaluate the respective contributions, the experimental data were fitted over the whole temperature range by

$$\chi_{exp} = C/T + \chi_{DIA} + \chi_o, \qquad [1]$$

where χ_{DIA} is the diamagnetic contribution of the atoms (-132×10^{-6} and -194×10^{-6} emu · mole^{-1} for $BaCu_2S_2$ and $BaCu_4S_3$, respectively), and χ_o is the temperature-

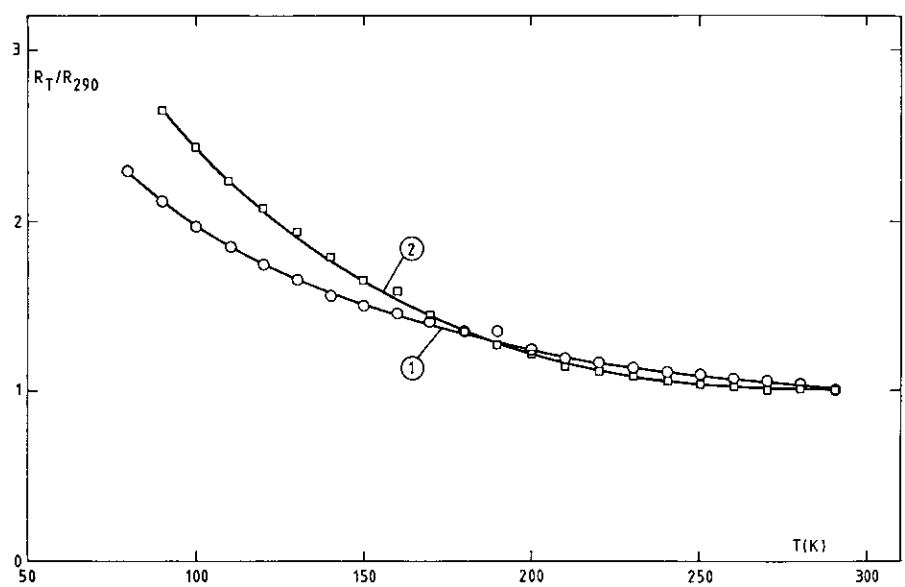

FIG. 3. Electrical resistivity (normalized to the 290-K value) as a function of temperature for $BaCu_4S_3$ (curve 1) and $BaCu_2S_2$ (curve 2).

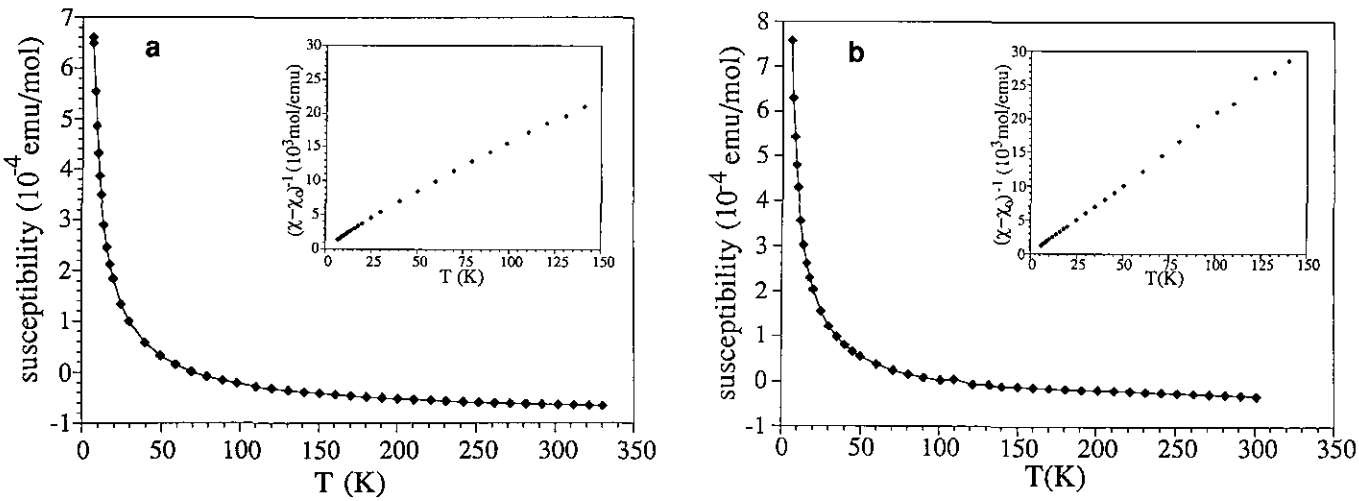

FIG. 4. Experimental magnetic susceptibility χ_{exp} and $1/(\chi - \chi_o)$ (insets) as a function of temperature T (K) for (a) $BaCu_2S_2$ and (b) $BaCu_4S_3$.

independent paramagnetism. The latter contribution has been determined by means of a linear correlation of $\chi * T$ versus T with $\chi = \chi_{exp} - \chi_{DIA}$ over the whole set of temperature available (5–300 K). Values of χ_o (53.3 ± 0.9) 10^{-6} and (167.0 ± 1.0) 10^{-6} emu · mole^{-1} are calculated for $BaCu_2S_2$ and $BaCu_4S_3$, respectively. The confidence limits have been determined for the calculation of χ_o with the corresponding numerical equation at the usual probability threshold of 0.05.

The insets in Figs. 4a and 4b show the inverse of the molar term $(\chi - \chi_o)^{-1}$ versus T over the temperature range 5–140 K (after substraction of the diamagnetic contribution) following

$$(\chi - \chi_o)^{-1} = T/C, \qquad [2]$$

supposing that the straight lines determined with the corresponding equations cut the origin, i.e., supposing that their intercept θ/C of a more exact Curie–Weiss law is negligible. This is not really the case, as a statistical test can show it. However, the value of C obtained this way is admitted to be the best averaged one. The Curie constants are then found to be $C = (5.83 \pm 0.05)\ 10^{-3}$ and $(4.20 \pm 0.04)\ 10^{-3}$ emu · K · mole^{-1} leading to very low magnetic moments μ_{eff} of 0.22 and 0.18 μ_B ($\approx$0.2 μ_B) for $BaCu_2S_2$ and $BaCu_4S_3$, respectively.

Supposing that the Curie constant for Cu^{2+} equals 0.374 emu · K · mol^{-1}, it is then possible to estimate the relative concentration n of copper atoms in a d^9 oxidation state, from the relation $n = 0.374/C$, where C are the experimental Curie constants. The negligible values obtained by this way (less than 1.5%) suggest that the paramagnetic increase is rather an impurity effect superposed to the intrinsic diamagnetic behavior of the two compounds.

(*d*) *Band Structure Calculations*

Extended Hückel calculations have been performed in order to interpret the electrical and magnetic properties of $BaCu_2S_2$ (18) and $BaCu_4S_3$.

1. The $BaCu_2S_2$ material. As said previously, the formal oxidation formalism appropriate for $BaCu_2S_2$ is $(Ba^{2+})[(Cu^+)_2(S^{2-})_2]^{2-}$. As mentioned earlier, the Cu_2S_2 layers contain only tetrahedrally coordinated copper atoms. With formal d^{10} ML_4 tetrahedra forming the slabs, $BaCu_2S_2$ should be an insulator (or a semiconductor). The density of states (DOS) of the 3-D material shown in Fig. 5 agrees with this statement. A gap of ca. 4 eV (probably somewhat overestimated, this is inherent to the calculation method) is computed between the valence and conduction bands. The shape of the DOS can easily be understood starting from the analysis of the orbitals of a d^{10} $(CuS_4)^{7-}$ fragment, which is the building block of the Cu_2S_2 layers. The usual molecular orbital pattern of a hypothetical tetrahedral $(CuS_4)^{7-}$ complex is illustrated on the left-hand side of Fig. 5 (19). Note that because the valence-shell ionization potentials (H_{ii}) of Cu 3*d* atomic orbitals (*AO*) are slightly below those of the S 3*p* *AO*s, the antibonding Cu–S molecular orbitals (*MO*) are slightly more localized on the sulfur atoms. The opposite situation occurs for the bonding Cu–S *MO*s. A large gap of 9.8 eV separates the $3t_2$ highest occupied molecular orbital (HOMO) from the $2a_1$ lowest unoccupied molecular orbital (LUMO), for a count of d^{10}. Rather strong covalent bonding is observed between Cu and S atoms, mainly due to bonding interaction of the vacant Cu *s* and *p* *AO*s with occupied S *s* and *p* *MO*s. The computed Cu–S overlap population is 0.324.

The DOS of $BaCu_2S_2$ should be deduced from this simple *MO* diagram. We just must take into account the

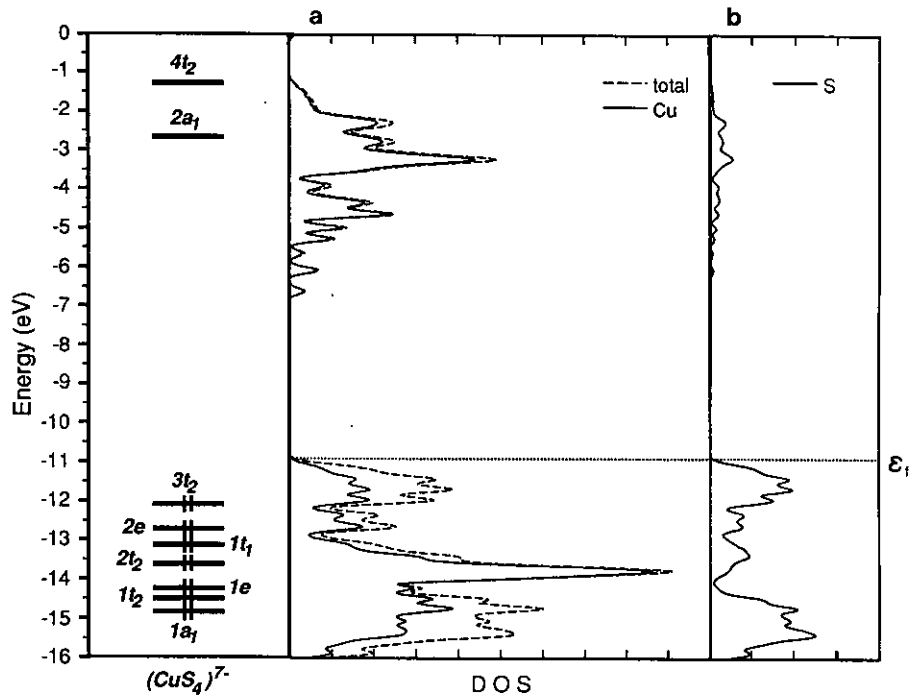

FIG. 5. DOS of $BaCu_2S_2$: (a) total DOS (dashed line) and Cu contribution (solid line); (b) S contribution. The *MO* levels of the isolated $(CuS_4)^{7-}$ fragment are recalled on the far left.

additional Cu–Cu interactions, which might occur. Indeed, in addition to a tetrahedral sulfur shell, each Cu atom is surrounded by a square of Cu congeners, distant of 2.76 Å (*vide supra*). Significant Cu–Cu interactions are expected at such separations. This is particularly the case for the σ-type *MO*s of a_1 and e symmetry. For instance, the $2a_1$ *MO* gives rise to one broad band spreading over 6 eV. The peaks around −12 eV derive from the Cu–Cu bonding and antibonding combinations of the $1e$ *MO* (see Fig. 5). Broad bands are also observed around −14 eV. The Cu–Cu interactions lead to a decrease of the HOMO–LUMO gap, which is now 4.2 eV (see Fig. 5). The electron transfer from the Ba atoms toward the Cu–S framework is almost complete. The computed atomic net charges are

$$(Ba^{1.60+})[(Cu^{0.11-})_2(S^{0.69-})_2]^{1.60-}.$$

These charges reflect the rather large ionic character of the interactions between the Ba atoms and the Cu_2S_2 slabs and the covalent character of that between copper and sulfur atoms inside the slabs. The Cu–S overlap population (0.266) is comparable to that computed in the molecular complex $(CuS_4)^{7-}$. An analysis of the Cu–S overlap population as function of the energy (20) indicates that the bottom of the valence band is strongly Cu–S bonding, whereas the top is Cu–S antibonding. This was expected from the analysis of the orbitals of the $(CuS_4)^{7-}$ monomer. The weakly positive Cu–Cu overlap population (0.021) is due to second-order mixing of the Cu 4*s* and 4*p* bonding states into occupied levels, since both Cu–Cu bonding and antibonding 3*d* states are occupied in the valence band (see Fig. 5). Note that the highly covalent character observed between copper and sulfur atoms in $BaCu_2S_2$ has already been noted both experimentally and theoretically (21, 22).

Surprisingly enough, LMTO-ASA band calculations very recently performed by Osadchii and colleagues show a very weak peak of DOS at the Fermi level mainly made of Ba and S participation (21). The authors conclude that the material should be metallic. This is somewhat puzzling to us. A drastic change of the Cu H_{ii} parameters and the introduction of Ba 5*d* levels, and S 3*d* levels do not change our conclusions. In any case, we do not find a metallic behavior for $BaCu_2S_2$, in agreement with the experimental results (*vide supra*).

The top of the valence band is Cu–Cu *and* Cu–S antibonding. Consequently, a removal of electrons would strengthen the Cu–Cu and Cu–S contacts. This would also render $BaCu_2S_2$ metallic. Such a situation could occur with a partial removal of Ba^{2+} cations in the lattice for instance. Cationic vacancies are often observed in solid-state copper chalcogenides. This is the case, for example, for $Na_{1.9}Cu_2Se_2$. Cu_2O, recently reported by Kanatzidis

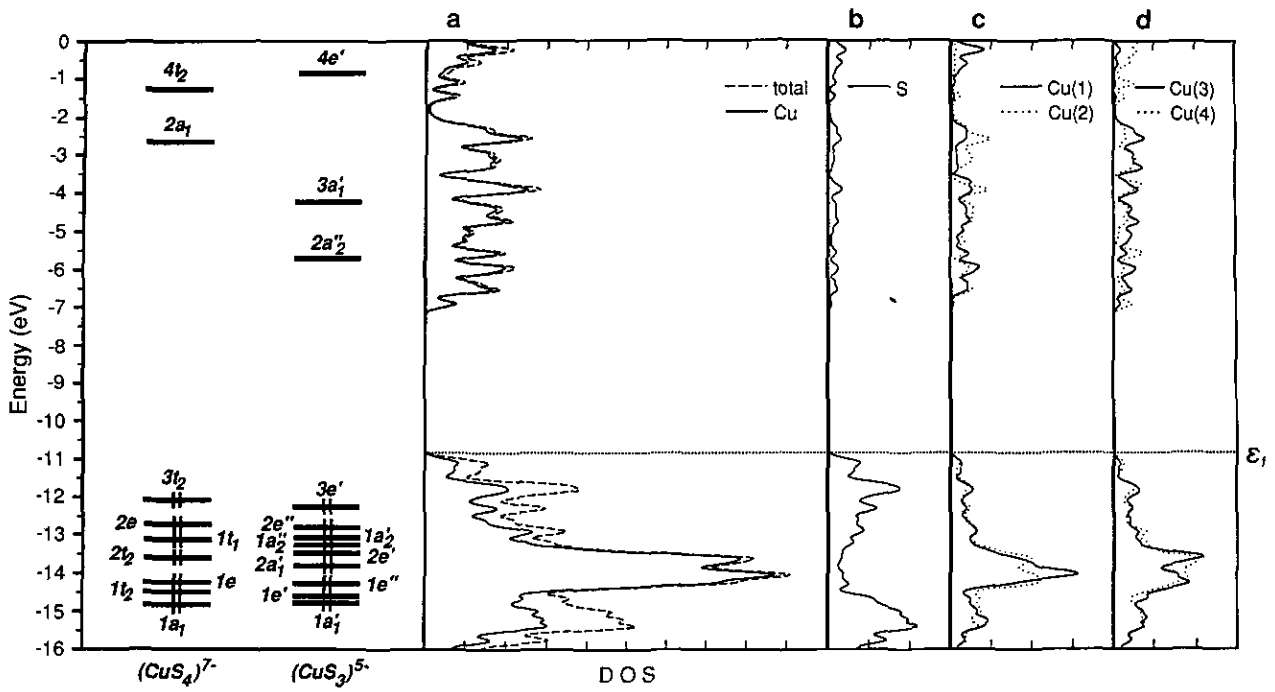

FIG. 6. DOS for $BaCu_4S_3$: (a) total DOS (dashed line) and Cu contribution (solid line); (b) S contribution; (c) contribution of copper atoms of types 1 (solid line) and 2 (dashed line); (d) contribution of copper atoms of types 3 (solid line) and 4 (dashed line). The *MO* levels of the isolated $(CuS_4)^{7-}$ and $(CuS_3)^{5-}$ fragments are recalled on the far left.

and co-workers (23). Alternatively, a partial replacement of Ba^{2+} cations by monovalent cations would also give rise to a conducting material as is the case for $TlCu_2Se_2$[3] of which the appropriate oxidation formalism is $Tl^+[Cu^+)(Cu^{2+})(Se^{2-})_2]^{-1}$ (24). $KCuFeS_2$ and $KCuFeSe_2$, recently reported by Mujica *et al.*, should also be metallic (16). Note finally that the arrangement observed in $BaCu_2S_2$, analog to that of $ThCr_2Si_2$, is rather scarce for d^{10} transition metals.

2. The $BaCu_4S_3$ material. Extended Hückel tight-binding calculations were carried out on the whole $BaCu_4S_3$ material. The formal oxidation state for the stoichiometric $BaCu_4S_3$ material is $(Ba^{2+})[(Cu^+)_4(S^{2-})_3]^{2-}$. Thus, $BaCu_4S_3$ containing d^{10} Cu^+ atoms should also be semiconducting. Indeed, a gap of 3.6 eV is computed between the valence and conduction bands, as shown in Fig. 6, where the DOS of $BaCu_4S_3$ is represented. As said previously, $BaCu_4S_3$ is made of distorted tetrahedral CuL_4 (Cu(3)) and almost planar Y-shaped CuL_3 fragments (Cu(1), Cu(2), and Cu(4)). The FMOs of regular tetrahedral $(CuS_4)^{7-}$ and Y-shaped $(CuS_3)^{5-}$ d^{10} entities are shown on the left-hand side of Fig. 6 (the distortion away from regular tetrahedral and trigonal environments, which is observed around the different Cu atoms in $BaCu_4S_3$ hardly perturbs the orbital patterns of the fragments). An important HOMO–LUMO gap (6.55 eV) is computed between the almost pure metal p a_2'' *MO* and the Cu–S antibonding $3e'$ *MO* for a d^{10} electron count. The Cu–S overlap population is slightly larger than that computed for $(CuS_4)^{7-}$ (0.366 vs 0.324).

According to the DOS, strong interactions occur between the different copper–sulfur fragments. Despite their different ligand environments, all copper atoms present comparable projected DOS (see Fig. 6). The metal–metal interactions lead to broad bands (particularly those deriving from the s and p Cu *MO*s). As a consequence, the calculated energy gap separating the valence and conduction bands (3.6 eV) is weaker than the HOMO–LUMO gaps observed in the $(CuS_4)^{7-}$ and $(CuS_3)^{5-}$ monomers (9.50 and 6.55 eV, respectively).

Rather strong positive overlap populations are computed for both Cu–S and Cu–Cu contacts. The Cu–S ones range from 0.07 to 0.426, depending on the distances (2.237–2.701 Å), and the Cu–Cu ones range from 0.003 (2.965 Å) to 0.046 (2.574 Å). As expected, the electron transfer from the Ba atoms toward the Cu–S framework is almost complete. The calculated atomic net charges are

$$(Ba^{1.58+})[(Cu(1)^{0.99-}Cu(2)^{0.04-}Cu(3)^{0.00}Cu(4)^{0.09-})(S(1)^{0.54-}S(2)^{0.33-}S(3)^{0.49-})]^{1.58-}.$$

If the compound was nonstoichiometric with some sulfur vacancies, it should be metallic due to some depopula-

[3] $TlCu_2S_2$ also exists (24). They both adopt the same structural arrangement as that of $BaCu_2S_2$.

tion of states lying in the top of the valence band. Then we may ask if we can predict the type of S atoms, which would be removed first. It turns out that the three types of sulfur atoms contribute to the top of the valence band. We note however, that they are not strictly identical since their atomic net charges differ somewhat (*vide supra*). As for $BaCu_2S_2$, another way to observe metallic conductivity for $BaCu_4S_3$ would be a partial removal of Ba^{2+} and also Cu^+ atoms.

Other ternary intercalated copper sulfides of stoichiometry 1 : 4 : 3 are known, such as KCu_4S_3 which crystallizes with a unique layered structure. Containing mixed-valence copper atoms (I, II), KCu_4S_3 is highly metallic (25).

CONCLUSION

The electrical properties reported here indicate that both $BaCu_2S_2$ and $BaCu_4S_3$ are semiconducting materials. Extended Hückel tight-binding calculations performed on stoichiometric compounds support this result and the Zintl concept can simply be used to rationalize the bonding observed in these materials. As expected then, $BaCu_2S_2$ and $BaCu_4S_3$ are diamagnetic. Further work is in progress in order to study the influence of the substitution of divalent Ba atoms by monovalent alkali metals, such as K or Cs, on the physical and electronic properties of $BaCu_2S_2$.

ACKNOWLEDGMENTS

Thanks are expressed to Dr. J. Padiou for the conductivity measurements, L. Ouahab for his help in single crystal studies, and L. Hubert for his expertise in the illustrations.

REFERENCES

1. J. E. Iglesias, K. E. Pachali, and H. Steinfink, *Mater. Res. Bull.* **7,** 1247 (1972).
2. J. E. Iglesias, K. E. Pachali and H. Steinfink, *J. Solid State Chem.* **9,** 6 (1974).
3. J. E. Iglesias and H. Steinfink, *Z. Kristallogr.* **142,** 398 (1975).
4. Z. Eliezer and H. Steinfink, *Mater. Res. Bull.* **11,** 385 (1976).
5. A. Ouammou, S. Le Mellay, J. Gaudé, P. Padiou, M. Mouallem-Bahout and C. Carel, *C.R. Acad. Sci. Paris Ser. II* **318,** 473 (1994).
6. M. Saeki, M. Onoda, and H. Nozaki, *Mater. Res. Bull.* **23,** 603 (1988).
7. M. Onoda and M. Saeki, *Mater. Res. Bull.* **24,** 1337 (1989).
8. M. V. Savel'eva, L. N. Trushnikova, A. A. Kamarzin, V. I. Alekseev, I. A. Baidina, S. V. Borisov, S. A. Gromilov, and A. G. Blinov, *Izv. Sib. Otd. Akad. Nauk SSSR Ser. Khim. Nauk* **3,** 157 (1989).
9. (a) M.-H. Whangbo and R. Hoffmann, *J. Am. Chem. Soc.* **100,** 6093 (1978); (b) M.-H. Whangbo, R. Hoffmann, and R. B. Woodward, *Proc. R. Soc. London Ser. A* **366,** 23 (1979).
10. R. Hoffmann, *J. Chem. Phys.* **39,** 1397 (1962).
11. R. Ramirez and M. C. Böhm, *Int. J. Quantum Chem.* **30,** 391 (1986).
12. P. Villars and L. D. Calvert, "Pearson's Handbook of Crystallographic Data for Intermetallic Phases," Vol. 2, p. 1668 ($BaCu_2S_2$), 1669 ($BaCu_4S_3$). ASM International, Materials Park, OH, 1991. J. L. C. Daams, P. Villars, and J. H. N. van Vucht, "Atlas of Crystals Structure Types for Intermetallic Phases," Vol. 2, p. 1924 ($BaCu_4S_3$: Pearson symbol oP32). ASM International, Materials Park, OH, 1991.
13. M. V. Savel'eva, V. I. Alekseev, L. N. Trushnikova, A. A. Kamarzin, I. A. Baidina, S. V. Borisov, S. A. Gromilov, and A. G. Blinov, *Izv. Sib. Otd. Akad. Nauk SSSR Ser. Khim. Nauk* **1,** 123 (1990).
14. M. V. Savel'eva, L. N. Trushnikova, A. A. Kamarzin, V. I. Alekseev, I. A. Baidina, S. V. Borisov, S. A. Gromilov, and A. G. Blinov, *Izv. Akad. Nauk SSSR Neorg. Mater.* **26,** 2653 (1990).
15. Z. Ban and M. Sikirica, *Acta Crystallogr.* **18,** 594 (1965).
16. C. Mujica, J. Paez, and J. Llanos, *Mater. Res. Bull.* **29,** 263 (1994).
17. O. V. Andreiev and N. N. Parshukov, *Zh. Neorg. Khim.* **36,** 2106 (1991).
18. For a complete theoretical study on the $ThCr_2Si_2$ type of compounds to which $BaCu_2S_2$ belongs to, see: (a) R. Hoffmann and C. Zheng, *J. Phys. Chem.* **89,** 4175 (1985); (b) C. Zheng, R. Hoffmann, and H.-G. von Schnering, *J. Am. Chem. Soc.* **108,** 1876 (1986); (c) C. Zheng and R. Hoffmann, *Z. Naturforsch. Sect. B* **41,** 292 (1986); (d) C. Zheng and R. Hoffmann, *J. Am. Chem. Soc.* **108,** 3078 (1986); (e) C. Zheng and R. Hoffmann, *J. Solid State Chem.* **72,** 58 (1988); (f) C. Zheng, *J. Am. Chem. Soc.* **115,** 1047 (1993).
19. T. A. Albright and J. K. Burdett and M. H. Whangbo, "Orbital Interactions in Chemistry." Wiley, New York, 1985.
20. (a) T. Hughbanks and R. Hoffmann, *J. Am. Chem. Soc.* **105,** 3528 (1983); (b) S. D. Wijeyesekara and R. Hoffmann, *Organometallics* **3,** 949 (1984); (c) M. Kertesz and R. Hoffmann, *J. Am. Chem. Soc.* **106,** 3483 (1984).
21. M. S. Osadchii, A. V. Okotrub, I. P. Asanov, V. V. Murakhtanov, and L. N. Mazalov, *Zh. Strukt. Khim.* **34,** 9 (1993).
22. M. S. Osadchii, E. A. Kravtsova, L. N. Mazalov, I. P. Asanov, G. K. Parygina, M. V. Savel'eva, and Yu. P. Dikov, *Zh. Strukt. Khim.* **33,** 68 (1992).
23. Y. Park, D. C. Degroot, J. L. Schindler, C. R. Kannewurf, and M. G. Kanatzidis, *Chem. Mater.* **5,** 8 (1993).
24. (a) R. Berger and C. F. van Bruggen, *J. Less-Common Met.* **99,** 113 (1984); (b) R. Berger, *J. Less-Common Met.* **147,** 141 (1989); (c) A. S. Avilov, R. M. Imanov, and Z. G. Pinsker, *Sov. Phys. Crystallogr. (Engl. Trans.)* **16,** 542 (1971).
25. (a) W. Rudorff, H. G. Schwarz, and M. Z. Walter, *Z. Anorg. Allg. Chem.* **269,** 141 (1952); (b) K. Klepp, H. Boller, and H. Völlekle, *Monatsch. Chem.* **111,** 727 (1978); (c) D. B. Brown, J. A. Zubieta, P. A. Vella, J. T. Wrobleski, T. Watt, W. E. Hatfield, and P. Day, *Inorg. Chem.* **19,** 1945 (1980).